

Supporting Information

Contents

	Page
Experimental	S2
Scheme S1	S6
Figures S1- S19	S7 – S18

Experimental

Materials. For the biological experiments, RPMI-1640, foetal bovine serum, L-glutamine, penicillin/streptomycin mixture, trypsin/EDTA, and phosphate-buffered saline (PBS) were purchased from GE Healthcare. Propidium iodide (>94%) and RNase A were obtained from Sigma Aldrich.

Synthesis of [Os(η^6 -*p*-cym)(Azpy-NMe₂)I]PF₆ (1**).** This complex was synthesized and characterized as described previously.¹

Cell Culture. A2780 human ovarian carcinoma cells were obtained from the European Collection of Cell Cultures (ECACC), used between passages 5 and 18 and grown in Roswell Park Memorial Institute medium (RPMI-1640) supplemented with 10% v/v of foetal calf serum, 1% v/v of 2 mM glutamine and 1% v/v penicillin/streptomycin. Cells were grown as adherent monolayers at 310 K in a 5% CO₂ humidified atmosphere and passaged at approximately 70-80% confluence.

Preparation of samples (whole cells). Silicon frames with silicon nitride windows (5x5 mm wide, 200 μ m thick silicon frames with 1.5x1.5 mm wide and 500 nm thick silicon nitride windows; Silson Ltd) were deposited on 24-well plates and irradiated with UV light for 20 min. Then, A2780 ovarian carcinoma cells were seeded (1×10^5 cells/well) and left to attach for 24 h in RPMI1640 medium. Samples were then treated with 1 μ M of **1**. After 24 h, cells were washed three times with PBS and ultrapure water. Excess liquid was blotted for 2 s using pin filter paper. Finally, samples were cryofixed in a propane-ethane mixture, dehydrated in a freeze dryer, and stored at room temperature in a clean desiccator until used.

Preparation of samples (sections). A2780 ovarian carcinoma cells were seeded in 100 mm petri dishes (5×10^6 cells/well) and left to attach for 24 h in RPMI1640 medium. Samples were then treated with 1 μ M **1**. After 24 h, cells were washed twice with PBS, and fixed for 20 min with 2% glutaraldehyde in sodium cacodylate buffer at pH 7.6 (Agar Scientific) for 1 h, with regular shaking. Then, cells were washed 3x with PBS, and transferred to Falcon tubes using a scrapper prior to centrifugation. Finally, cells were dehydrated with graded levels of ethanol (20-100% ethanol), and then infiltrated with 100% propylene oxide for 1 h followed by a 1:1 mixture of propylene oxide and

EPON resin for 6 h. This was replaced with several changes of 100% resin over 18 h before curing for 24 h at 333 K. Blocks were trimmed and sectioned on a Leica Ultracut E ultramicrotome (Leica Microsystems). Sections 500 nm thick were collected on appropriate sample holders for XRF (5x5 mm wide, 200 μm thick silicon frames with 1.5x1.5 mm-wide and 500 nm-thick silicon nitride windows; Silson Ltd), and then imaged according to requirements.

Beamline settings: The beam was focused to 70x100 nm² using KB mirrors (Si substrates coated with graded W/B4C multilayers). The irradiation energy for of the samples during acquisition of XRF maps or XAS spectra was controlled with a fixed exit double Si(111) crystal monochromator (Kohzu; Japan), and detection was achieved using a pair of 3-element silicon drift detectors (RaySpec Ltd., UK).

Acquisition of XRF maps: XRF experiments were performed on the ID16B beamline at the ESRF synchrotron light source. Irradiation of the samples was done with a monochromatic beam of 11.2 keV energy, and a flux of 5x10⁸ ph/s. Scan step size was fixed at 1000x1000 nm² (dwell time 1 s) for coarse scans and 100x100 nm² (dwell time 1s) for fine scans. Spectra were fitted using the free PyMCA software.²

Image Analysis: Images were opened and processed using FIJI ImageJ package³ with the EDFread plugin.

Nano-XAS acquisition: XAS spectra were collected at ID16B in areas identified in the XRF maps as having the highest concentration of Os. Spectra were collected at ambient temperature with a focused beam (70x100 nm²) in fluorescence mode. Acquisition started 50 eV before the expected Os-L_{III} edge and finished 250 eV after (10.82-11.12 keV; corresponding to a K-range up to about 8 \AA^{-1}), and used 1 eV step-size with 3 s accumulation (flux: 5x10⁸ ph/s). Several XAS scans were acquired on the areas studied to check reproducibility of the spectra and improve the signal to noise ratio. The position of the beam was realigned before each scan, as some level of vertical drift was expected due to the non-perfect rotation of the monochromator used (approx. 50 nm over an energy scan of 250 eV). 4 standards for Os in different oxidation states were measured at the end of the run. XAS spectra for 4 additional standards - Os II compounds with different ligands - were collected at B18 beamline (Diamond). The measurement of one of the standards was repeated in order to be

able to apply the right energy calibration and correct for the different offsets introduced by the two beamlines.

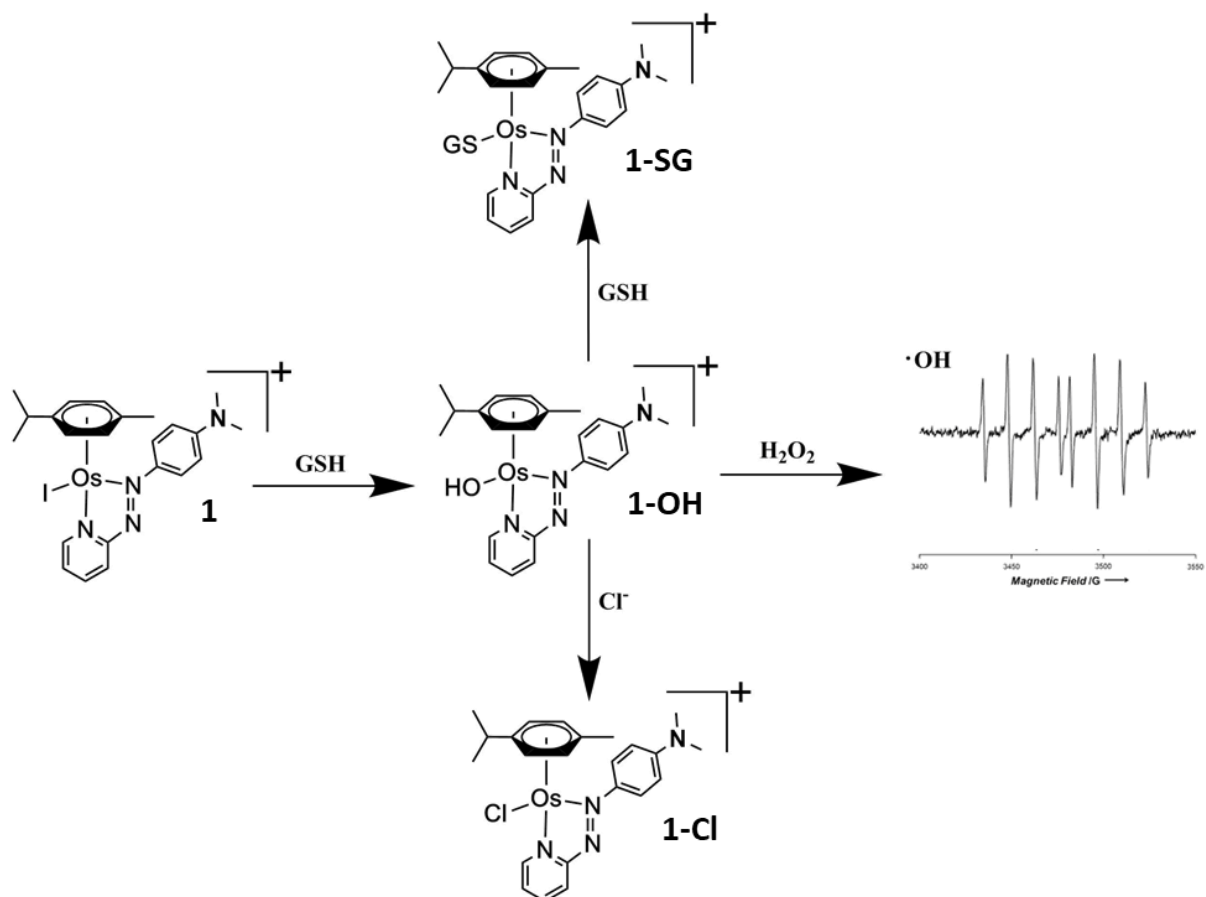
XAS spectra Analysis: XANES data were normalized by means of a custom made python script using a constant value for the pre-edge evaluation and a 2nd order polynomial function for the post –edge. This was done because the Athena software⁴ does not allow to use a 0-order function for the pre-edge subtraction, which was necessary in our case due to the short energy range and low fluorescence count rate of the data acquired. XANES spectra were then opened and processed using the Athena software.⁴ The normalized data were compared to data measured on Os standards in transmission mode in order to verify that the normalization was performed correctly. Scans collected on the same sample point have been averaged to improve the signal to noise ratio.

Linear combination fits (using Os^{II} and Os^{III} standards) were performed on the averaged data to evaluate the relative amount of different Os oxidation states in the sample. This was done in python by means of `scipy.optimize.leastsq()` function, where the difference between experimental and fit was defined as $\text{exp_y(en)} - (a1 \cdot \text{refOs2(en)} + a2 \cdot \text{refOs3_y(en)})$ along the whole energy axis (en) used for the data collection. `refOs2` and `refOs3` were two functions obtained by the interpolation of the normalized experimental data collected for the references using the function `scipy.interpolate.splrep()`. Optimised parameters `a1` and `a2` were forced to stay within 0 and 1, and add to a total of 1. Errors were calculated from the diagonal elements of the covariance matrix resulting from the `leastsq()` function.

For the treatment of EXAFS data, we used of Viper software (*VIPER*, freeware).⁵ EXAFS signals were obtained after background removal with a smoothing spline passing through 8 knots and then the k^2 -weighted $\chi(k)$ function was Fourier transformed with a K-range from 1.5 to 8 Å⁻¹.

References

1. Y. Fu, A. Habtemariam, A. M. Pizarro, S. H. van Rijt, D. J. Healey, P. A. Cooper, S. D. Shnyder, G. J. Clarkson, P. J. Sadler, *J. Med. Chem.*, 2010, **53**, 8192.
2. V. A. Solé, E. Papillon, M. Cotte, P. Walter, and J. Susini, *Spectrochim. Acta B*, 2007, **62**, 63.
3. J. Schindelin, I. Arganda-Carreras, E. Frise, V. Kaynig, M. Longair, T. Pietzch, S. Preibisch, C. Rueden, S. Saalfeld, B. Schmid, J.-Y. Tinevez, D.J. White, V. Hartenstein, K. Eliceiri, P. Tomancak, A. Cardona, *Nat. Methods*, 2012, **9**, 676.
4. B. Ravel, M. Newville, *J. Synchrotron Rad.*, 2005, **12**, 537.
5. K. V. Klementev, *J. Phys. D. Appl. Phys.*, 2001, **34**, 209.
6. R.J. Needham, C. Sanchez-Cano, X. Zhang, I. Romero-Canelón, A. Habtemariam, M.S. Cooper, L. Meszaros, G.J. Clarkson, P.J. Blower and P.J. Sadler, *Angew. Chem. Int. Ed.*, 2017, **56**, 1017



Scheme S1. Activation of **1** in presence of GSH generating **1-OH**, and known reactions of the hydroxido reactive adduct with biologically available Cl^- , GSH or hydrogen peroxide.⁶

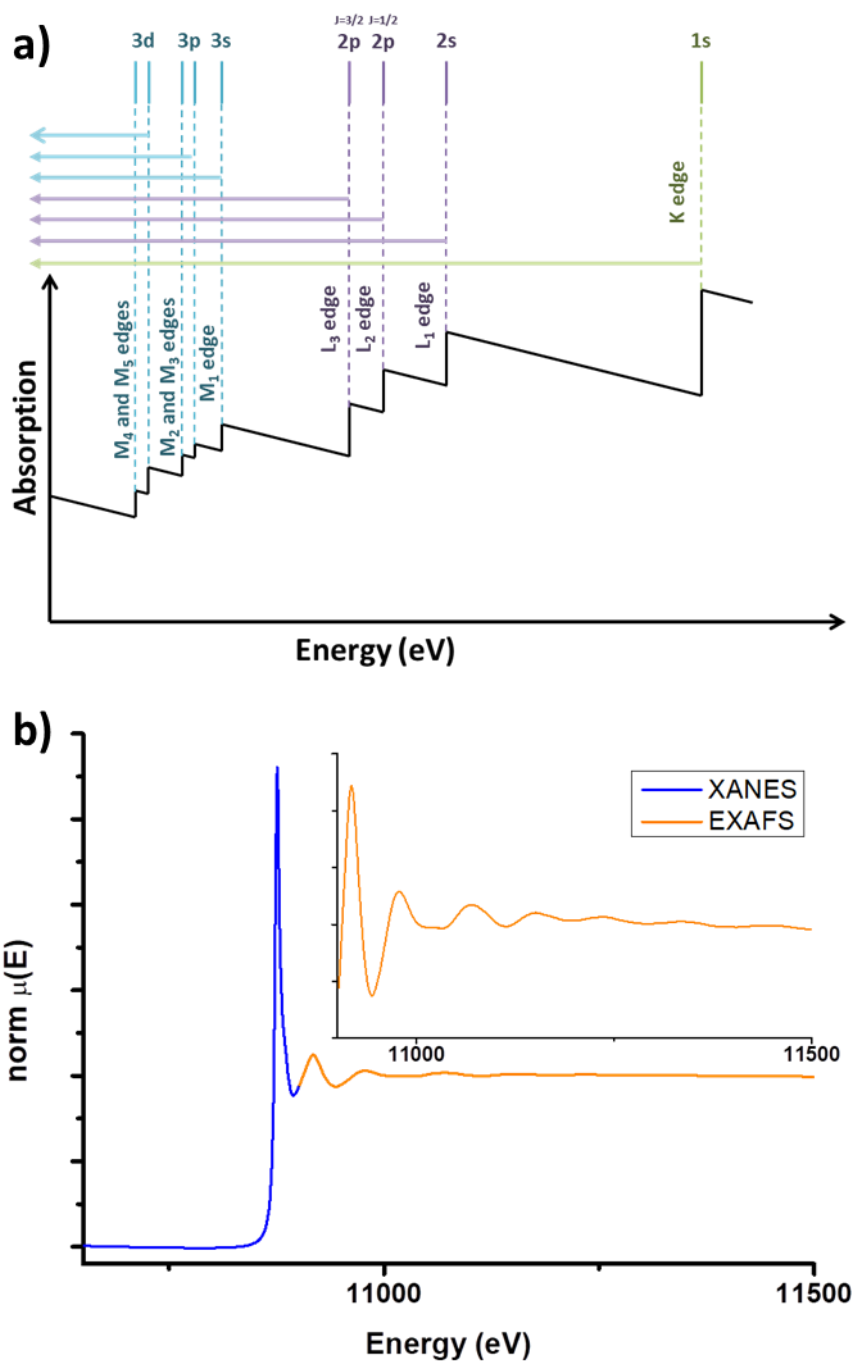


Figure S1. a) Scheme showing the typical X-ray absorption pattern of an element and the electronic transitions that contribute to X-ray Absorption spectroscopy (XAS). b) XAS spectrum highlighting the X-ray Absorption Near Edge Structure (XANES; blue line) area (including the pre-edge and edge areas), and Extended X-Ray Absorption Fine Structure (EXAFS; orange line) area (augmented in the overlapped insert).

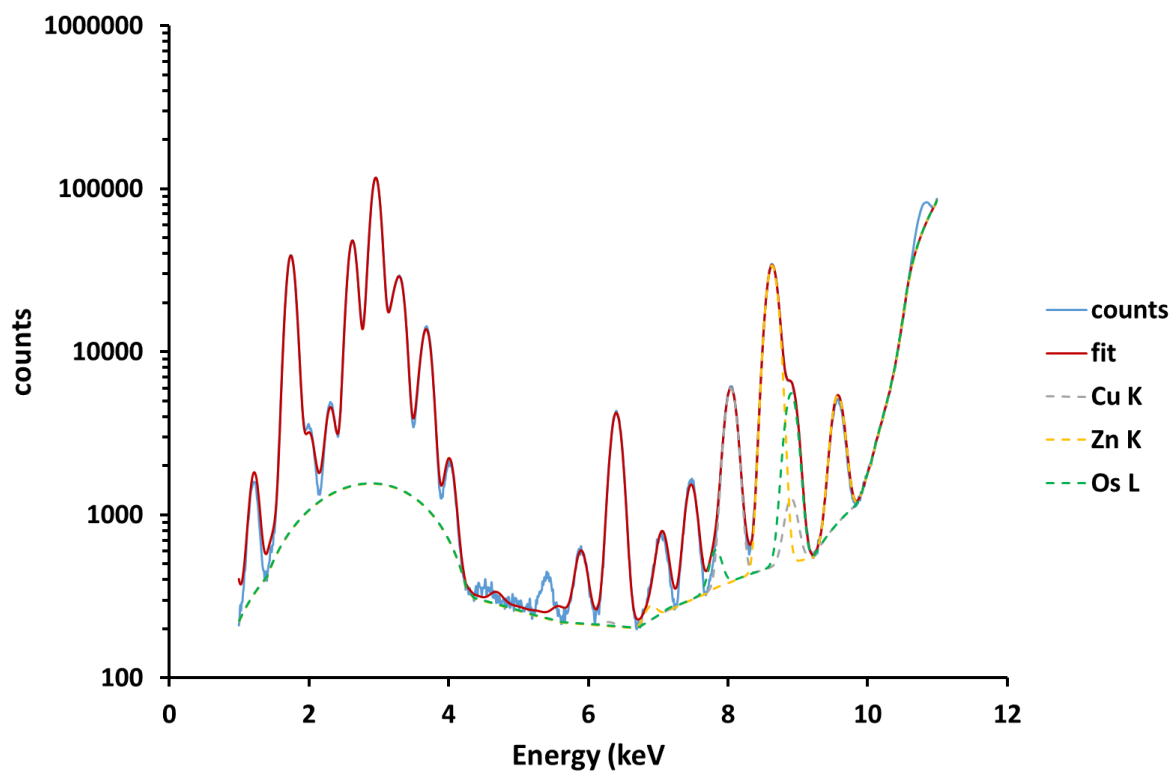


Figure S2. Normalised XRF spectrum from a whole A2780 cell treated with 1 μM (IC_{50}) of complex **1** for 24 h; Raster scan: 100x100 nm² step size, 1000 ms dwell time. The spectrum was fitted using PyMca,³ and the contribution of selected elements is displayed: Cu and Zn K x-ray emission lines, and Os L X-ray emission lines.

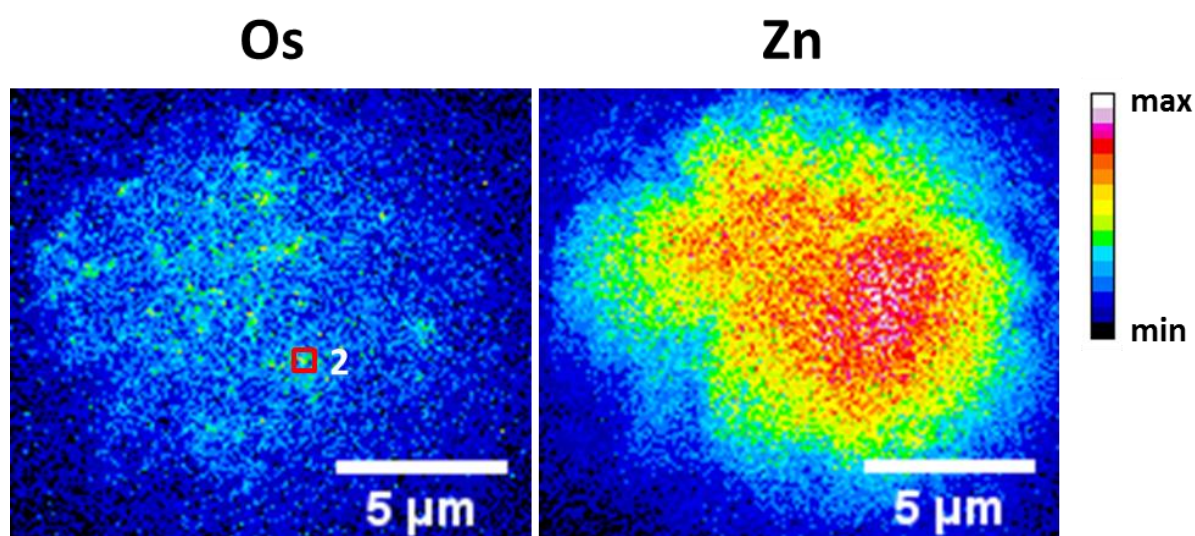


Figure S3. XRF maps of a cryofixed and dehydrated A2780 cell treated for 24 h with 1 μM **1** showing the cellular distribution of Os and Zn. Red squares and white numbers indicate areas where nano-XAS were collected. Raster scan: 100x100 nm² step size, 1 s dwell time.

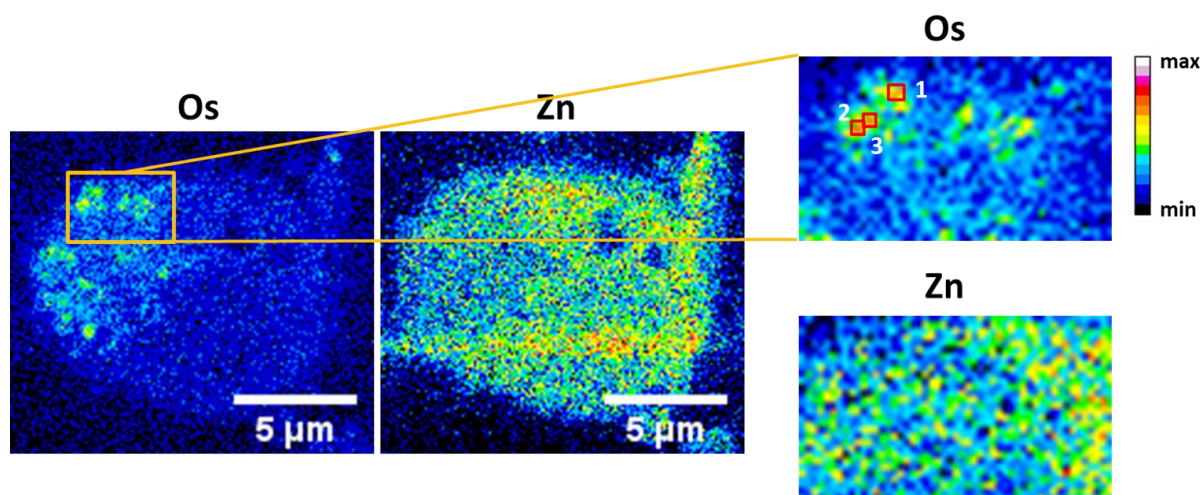


Figure S4. XRF maps of a 500 nm thick section of A2780 cell treated for 24 h with 1 μM **1** showing the cellular distribution of Os and Zn. Red squares and white numbers indicate areas where nano-XAS were collected. Raster scan: 100x100 nm² step size, 1s dwell time.

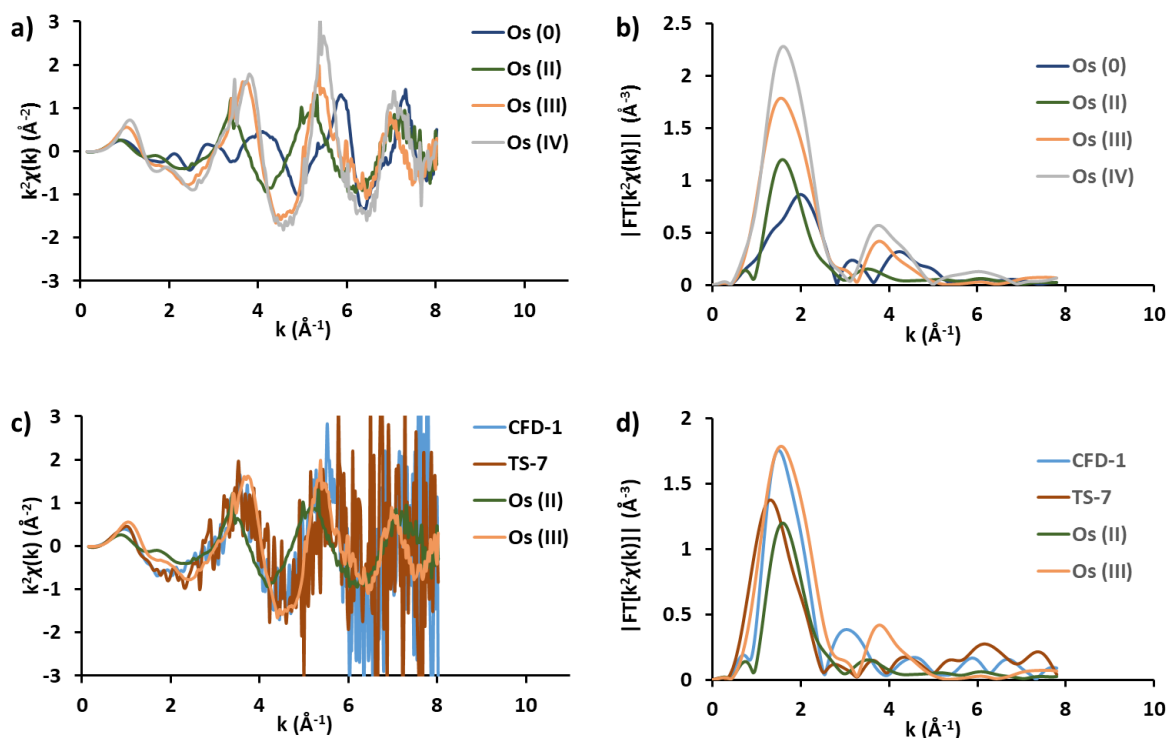


Figure S5. EXAFS functions for the Os standards: Os powder (Os^0), **1** (Os^{II}), OsCl_3 (Os^{III}) and $[\text{NH}_4]_2\text{OsCl}_6$ (Os^{IV}); a) k^2 -weighted $k^2\chi(k)$ and b) Phase-uncorrected magnitude part of the Fourier Transformed (FT-). EXAFS functions of **1** (Os^{II}) and OsCl_3 (Os^{III}) standards, and spectra collected in positions CFD-1, and TS-7; c) k^2 -weighted $k^2\chi(k)$ and d) Phase-uncorrected magnitude part of the Fourier Transformed (FT-). Scan: 10.82-11.12 keV; 1eV step; 3 s accumulation; 70x100 nm² beam size.

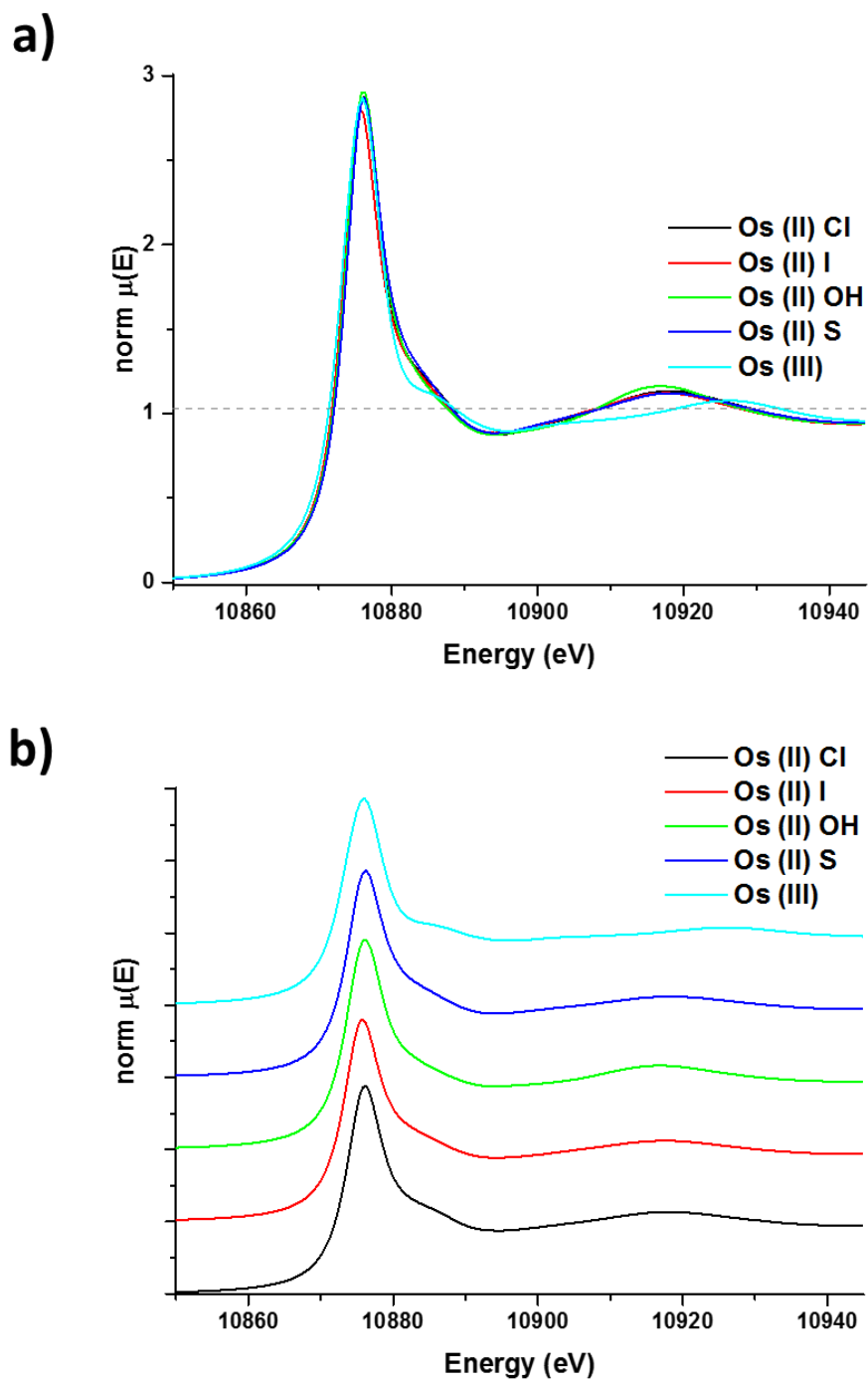


Figure S6. XANES spectra of Os^{II} standards: 1-Cl (Os^{II} Cl), **1** (Os^{II} I), 1-OH (Os^{II} OH), and 1-SG (Os^{II} S); and OsCl₃ (Os^{III}) showed as a) overlay or b) stack of the spectra. Scan: 10.82-11.12 keV; 1eV step; 3 s accumulation; 70x100 nm² beam size.

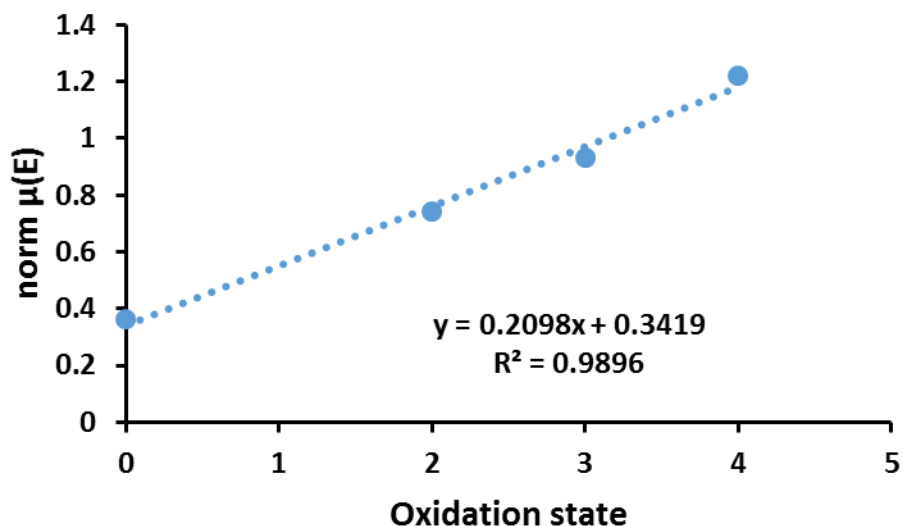


Figure S7. Correlation between the XAS absorption at 10871 eV (as norm $\mu(E)$) and oxidation state of Os. Obtained from XANES spectra of Os standards: Os powder (Os^0), **1** (Os^{II}), OsCl_3 (Os^{III}) and $[\text{NH}_4]_2\text{OsCl}_6$ (Os^{IV}).

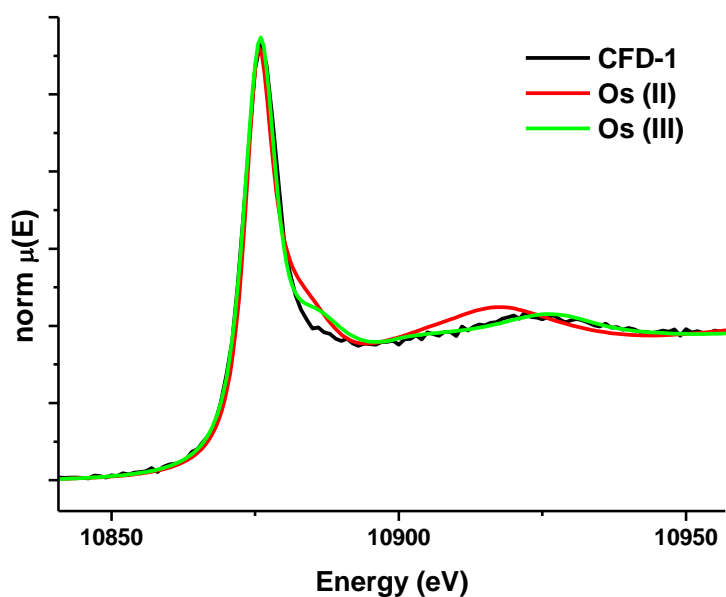


Figure S8. XANES spectra of **1** (Os^{II}) and OsCl_3 (Os^{III}) standards, and spectrum collected in position CFD-1. Scan: 10.82-11.12 keV; 1eV step; 3 s accumulation; $70 \times 100 \text{ nm}^2$ beam size.

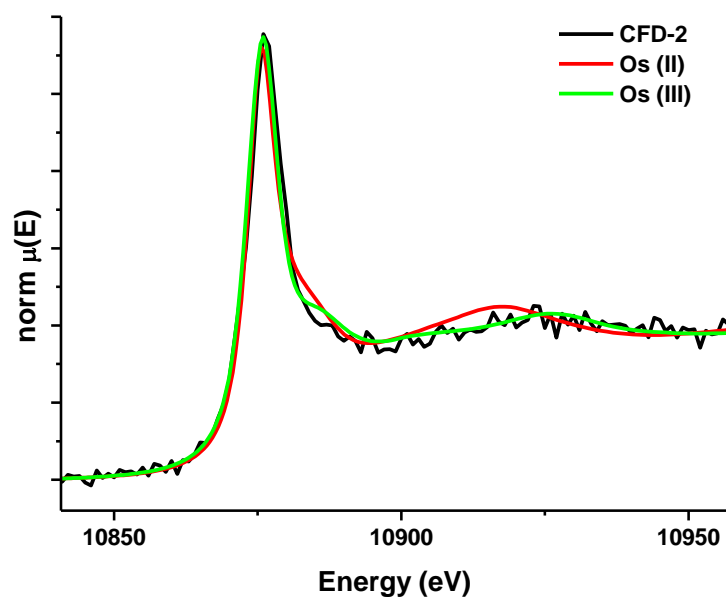


Figure S9. XANES spectra of **1** (Os^{II}) and OsCl₃ (Os^{III}) standards, and spectrum collected in position CFD-2. Scan: 10.82-11.12 keV; 1 eV step; 3 s accumulation; 70x100 nm² beam size.

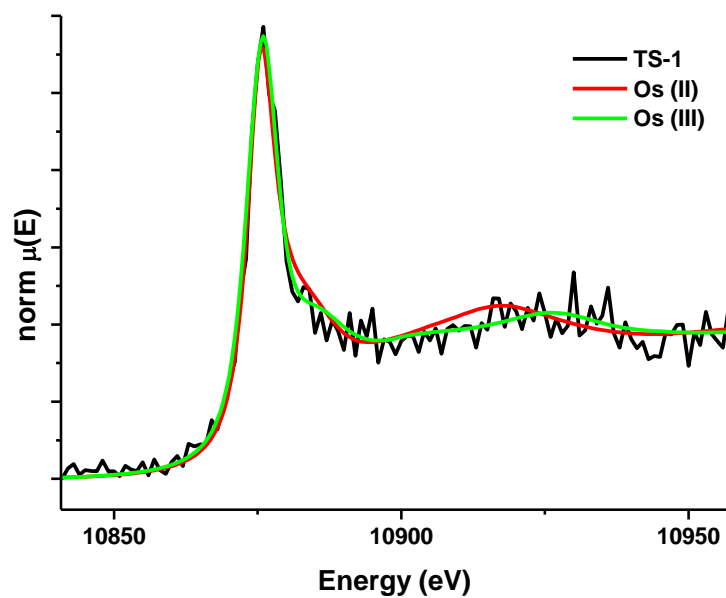


Figure S10. XANES spectra of **1** (Os^{II}) and OsCl₃ (Os^{III}) standards, and spectrum collected in position TS-1. Scan: 10.82-11.12 keV; 1 eV step; 3 s accumulation; 70x100 nm² beam size.

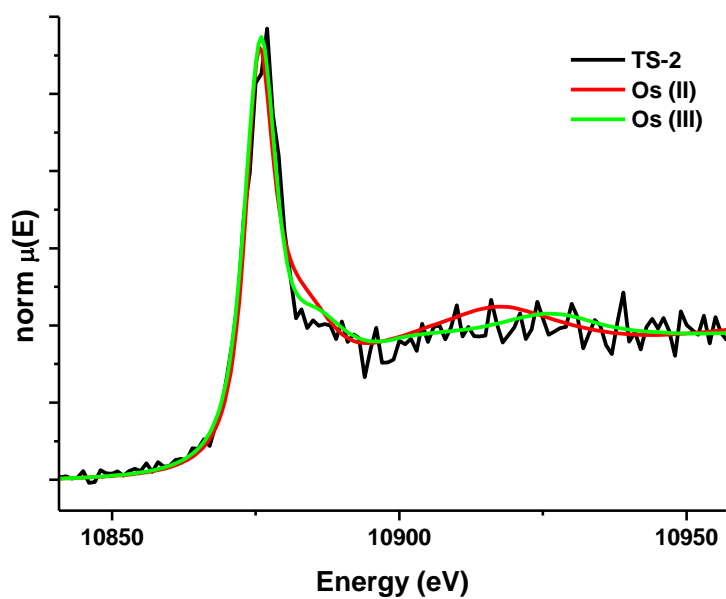


Figure S11. XANES spectra of **1** (Os^{II}) and OsCl₃ (Os^{III}) standards, and spectrum collected in position TS-2. Scan: 10.82-11.12 keV; 1 eV step; 3 s accumulation; 70x100 nm² beam size.

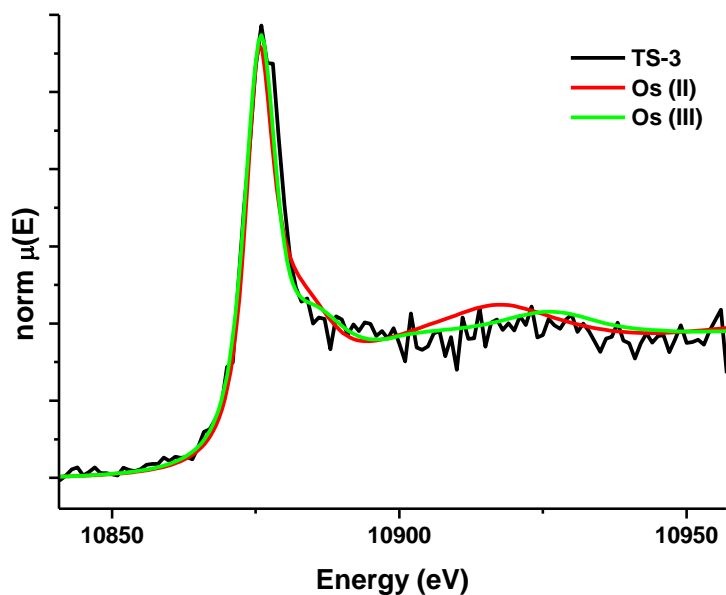


Figure S12. XANES spectra of **1** (Os^{II}) and OsCl₃ (Os^{III}) standards, and spectrum collected in position TS-3. Scan: 10.82-11.12 keV; 1 eV step; 3 s accumulation; 70x100 nm² beam size.

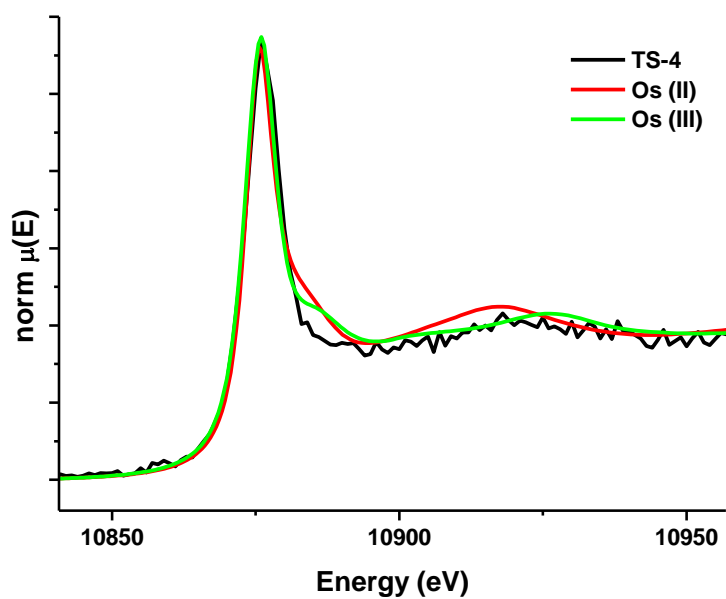


Figure S13. XANES spectra of **1** (Os^{II}) and OsCl₃ (Os^{III}) standards, and spectrum collected in position TS-4. Scan: 10.82-11.12 keV; 1 eV step; 3 s accumulation; 70x100 nm² beam size.

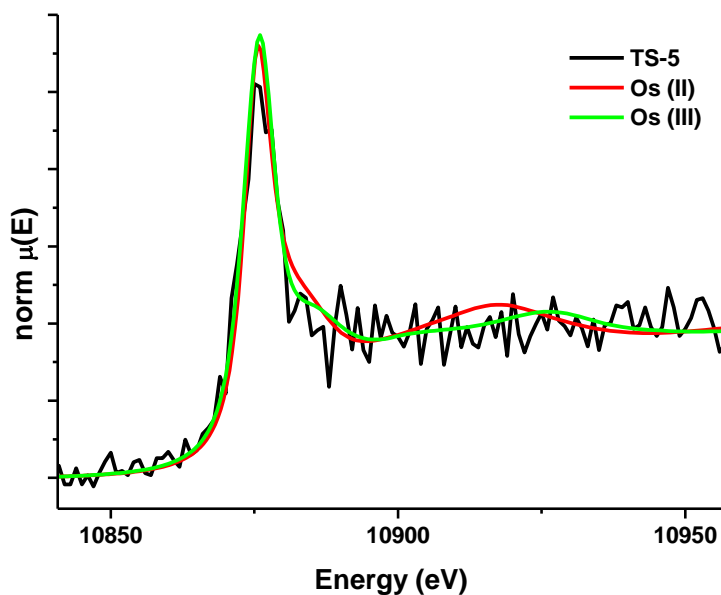


Figure S14. XANES spectra of **1** (Os^{II}) and OsCl₃ (Os^{III}) standards, and spectrum collected in position TS-5. Scan: 10.82-11.12 keV; 1 eV step; 3 s accumulation; 70x100 nm² beam size.

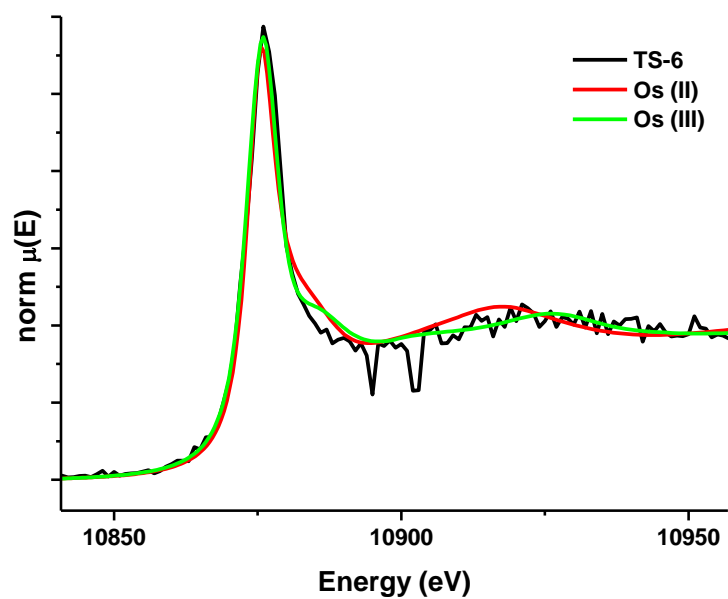


Figure S15. XANES spectra of **1** (Os^{II}) and OsCl₃ (Os^{III}) standards, and spectrum collected in position TS-6. Scan: 10.82-11.12 keV; 1 eV step; 3 s accumulation; 70x100 nm² beam size.

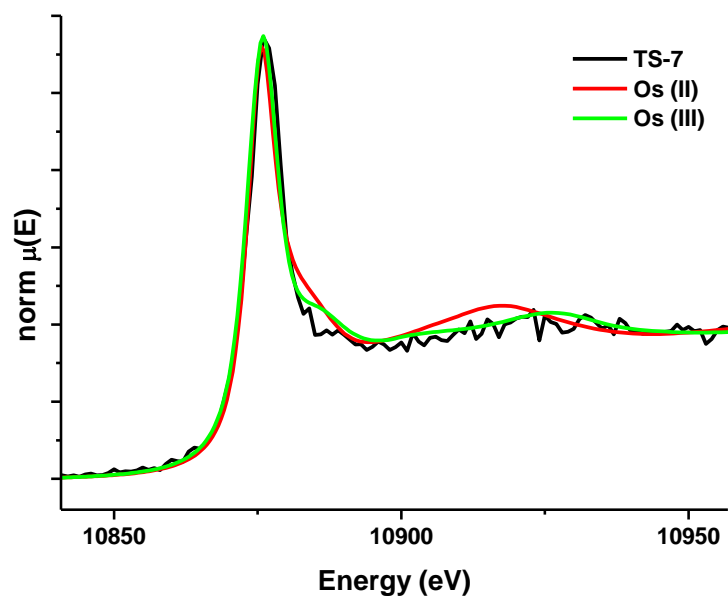


Figure S16. XANES spectra of **1** (Os^{II}) and OsCl₃ (Os^{III}) standards, and spectrum collected in position TS-7. Scan: 10.82-11.12 keV; 1 eV step; 3 s accumulation; 70x100 nm² beam size.

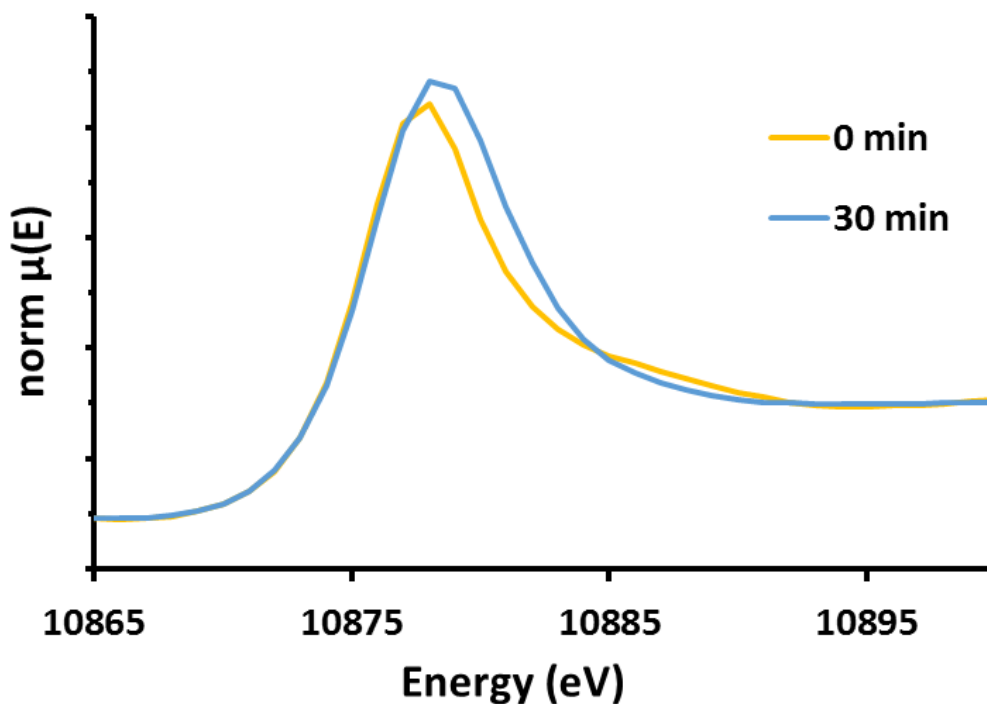


Figure S17. XANES spectra collected from a single standard of **1** showing beam damage towards higher oxidation states after irradiation of the sample for 30 min with a microfocused beam focused to $2 \times 2 \mu\text{m}^2$ (flux 2.4×10^{11} ph/s).

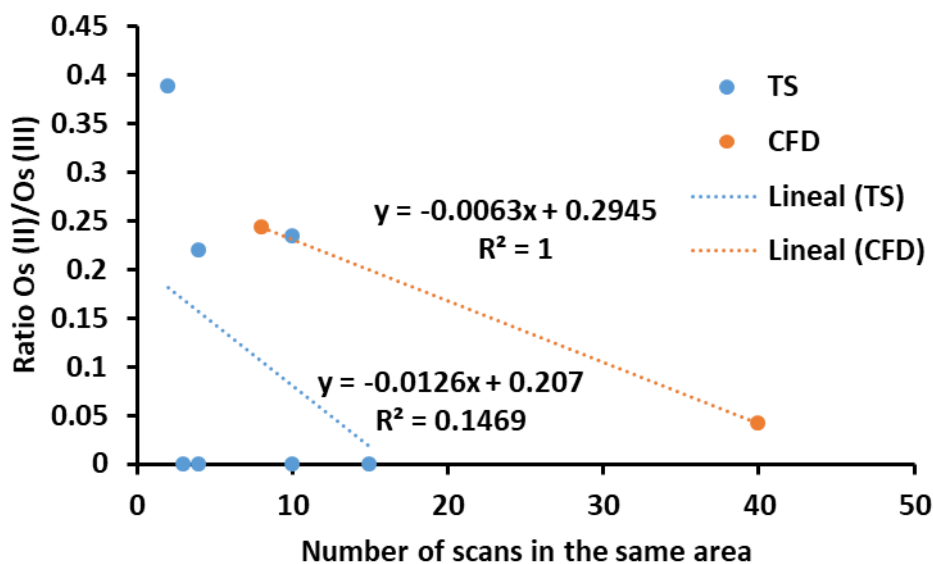


Figure S18. Possible correlation between quantity of Os(II) found for individual areas studied (calculated by LCF from XANES spectra) and number of scans collected. CFD indicate analysis of areas from cryofixed and dehydrated A2780 cells, while TS indicate analysis of areas from 500 nm thick sections of A2780 cells. Scan (each): 10.82-11.12 keV; 1eV step; 3 s accumulation; $70 \times 100 \text{ nm}^2$ beam size.

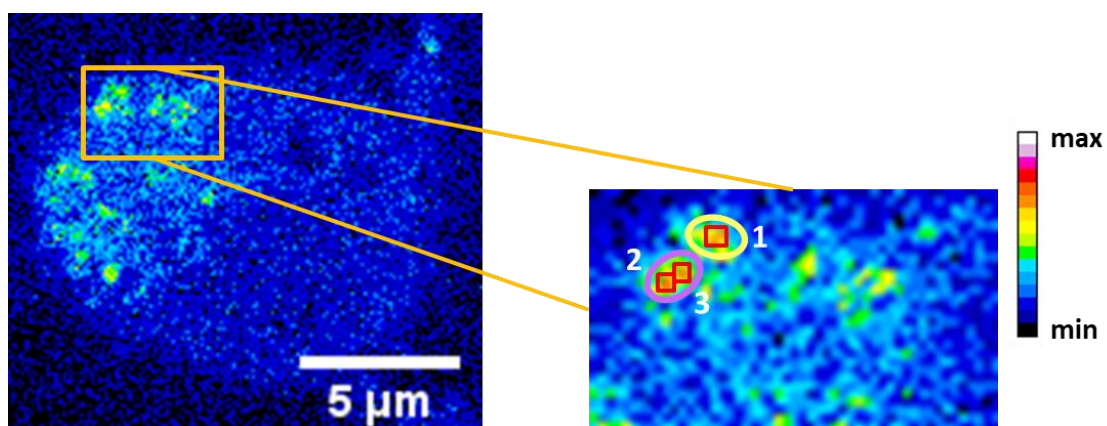


Fig.S19. XRF maps of 500 nm thick sections of a A2780 cell treated for 24 h with 1 μM **1** showing the cellular distribution of Os. Red squares and white numbers indicate areas where nano-XAS were collected. Purple ellipses indicate areas with 100% Os^{III} species. Yellow ellipses indicate areas with 20% Os^{II} species and 80% Os^{III} species. Raster scan: 100x100 nm^2 step size, 1s dwell time.